Supplementary Material

Shape Transformations of Soft Matter Governed by Bi-Axial Stresses

Héloïse Thérien-Aubin,[1] Michael Moshe,[2] Eran Sharon,[2] and Eugenia Kumacheva[1,3,4,*]
[1]*University of Toronto, Department of Chemistry, 80 Saint George street, Toronto, Ontario, M5S 3H6, Canada*
[2]*Hebrew University, The Racah Institute of Physic, Jerusalem, Israel*
[3]*University of Toronto, Department of Chemical Engineering and Applied Chemistry, 200 College Street, Toronto, Ontario M5S 3E5, Canada.*
[4]*University of Toronto, The Institute of Biomaterials and Biomedical Engineering, 4 Taddle Creek Road, Toronto, Ontario M5S 3G9, Canada*

S1. Experimental section

Materials. All chemicals were purchased from Sigma-Aldrich, unless specified. Monomers *N*-isopropylacrylamide (NIPAM), *N*,*N*'-methylene-*bis*-acrylamide (MBA), 2-acrylamido-2-propane sulfonic acid (AMPS), acrylamide (AA), and 2-2-azo-*bis*(2-methylpropionamidine)dihydrochloride (V-50) (Acros) were recrystallized before use. Butyl methacrylate (BMA) and *N*-hydroxyethylacrylamide (HEAM) were purified by column filtration over aluminum oxide.

Synthesis of poly(N-isopropyl acrylamide) primary gel (p(NIPAM). An aqueous monomer solution containing 14 wt% NIPAm, 1wt% MBA and 1 wt% V-50 was placed into a reaction cells built from two glass plates (6" × 3") separated with a silicone rubber spacer with a particular thickness and photopolymerized by exposing the solution to UV-irradiation (Hönle UVA print 9 mW/cm^2) for 25 sec. Following this step, 3"× 2" sheets were cut from the p(NIPAM) primary gel (PG) base sheet and washed in 750 mL of deionized water for 24 h (changed every 8 h).

Synthesis of p(NIPAM)/poly(2-acrylamido-2-propane sulfonic acid) patterned binary gel (p(NIPAM)/p(AMPS). The p(NIPAM) sheets were swollen for 18 h in a 250 mL of a aqueous monomer solution containing 20 wt% AMPS, 0.25wt% MBA and 0.5wt% V-50. The swollen gel was introduced

into a reaction cell and exposed for 30 s to UV-irradiation through a photomask printed on a transparency. The interpenetrating network (IPN) was formed in the light-exposed regions of the swollen gel, thereby forming the features of the binary gel (BG). Subsequently, the gel sheets were washed in 750 mL of water (changed every 8 h) for 24 h to remove unreacted reagents and linear, non-crosslinked polymers.

Synthesis of poly(acrylamide-co-butyl acrylate) primary gel (p(AA-co-BMA). The p(AA-*co*-BMA) primary gel sheet was prepared by photopolymerization by exposing a solution containing 15 wt% of a monomer mixture (60 mol% of AA and 40 mol% of BMA), 5 wt% of MBA, and 1 wt% of V-50 in a water-DMF mixture (40/60 v%) to UV irradiation for 45 sec. The gel sheets were cut in 3"ß 2" coupons and washed for 24 h in 750 mL of water-DMF mixture, which was changed every 8h, to remove any traces of unreacted monomers.

Synthesis of p(AA-co-BMA)/poly(N-isopropylacrylamide)/ poly(N-isopropylacrylamide-co-N-hydroxyethylacrylamide) binary gel (p(AA-co-BMA)/p(NIPAM)/p(NIPAM-co-HEAM). The p(AA-*co*-BMA) PG sheets were swollen for 18 h in 250 mL of an aqueous solution of 1 wt% of MBA, 1 wt% of V-50, and 15 wt% of NIPAM. The swollen gel was introduced into a reaction cell and exposed for 45 s to UV-irradiation through a photomask printed on a transparency, thereby forming BG-1 domains of the interpenetrating network of p(AA-*co*-BMA) and p(NIPAM). The gel sheets were washed in 750 mL of water (changed every 8 h) for 24 h to remove unreacted reagents and linear, non-crosslinked polymers. The patterned sheet of p(AA-*co*-BMA)/p(NIPAM) was then swollen for 18h in 250 mL in an aqueous solution of 1 wt% of MBA, 1 wt% of V-50, and 15 wt% of a monomer mixture composed of 75 mol% of NIPAM and 25 mol% of HEAM. The swollen gel was introduced into a reaction cell and exposed for 45 s to UV-irradiation through a second photomask printed on a transparency forming the BG-2 domains made of the interpenetrating network of p(AA-*co*-BMA) with p(NIPAM-*co*-HEAM). The gel sheets were washed in 750 mL of water (changed every 8 h) for 24 h to remove unreacted reagents and linear, non-crosslinked polymers.

S2. Evolution of double curvature shapes

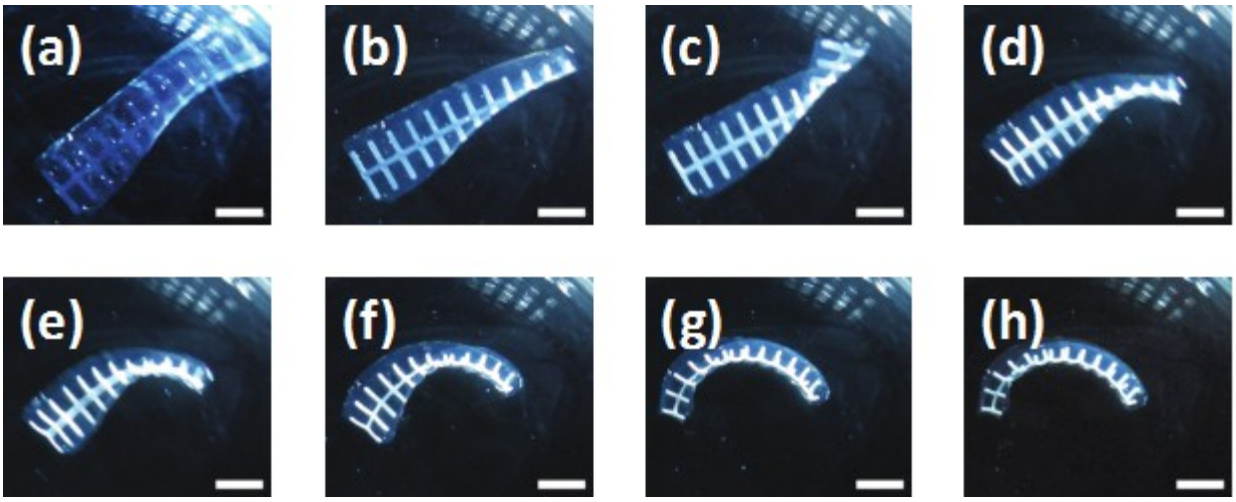

Fig. S1. Formation of the double curvature shape from a planar gel sheet. The p(NIPAM) (PG) sheet is patterned with the longitudinal and transverse lines of p(NIPAM)/p(AMPS) (BG) and transferred from water into in 1.5M NaCl solution for (a) 15 sec, (b) 5 min, (c) 10 min, (d) 30 min, (e) 60 min, (f) 90 min, g) 120 min, and (h) 300 min. The white color domains correspond to the contracted PG regions. The scale bar is 1 cm.

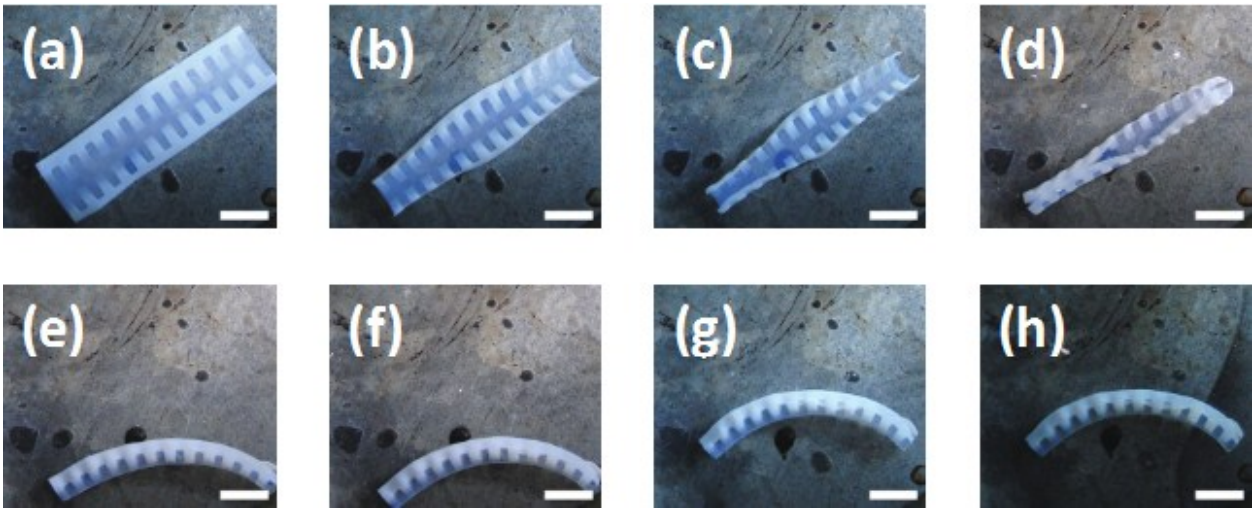

Fig. S2. Formation of the double curvature shape from a planar gel sheet. The p(AA-*co*-BMA) non-responsive PG sheet is patterned with transverse lines of temperature-responsive p(AA-*co*-BMA)/p(NIPAM) (BG-1) and the longitudinal stripe of temperature-responsive p(AA-*co*-BMA)/ p(NIPAM-*co*-HEAM) (BG-2), each with a different LCST. The sheet is immersed in water at 70°C for (a) 15 sec, (b) 5 min, (c) 10 min, (d) 15 min, (e) 20 min, (f) 30 min, (g) 60 min, (h) 120 min. The white color corresponds to the contracted BG-1 and BG-2 regions. The scale bar is 1 mm.

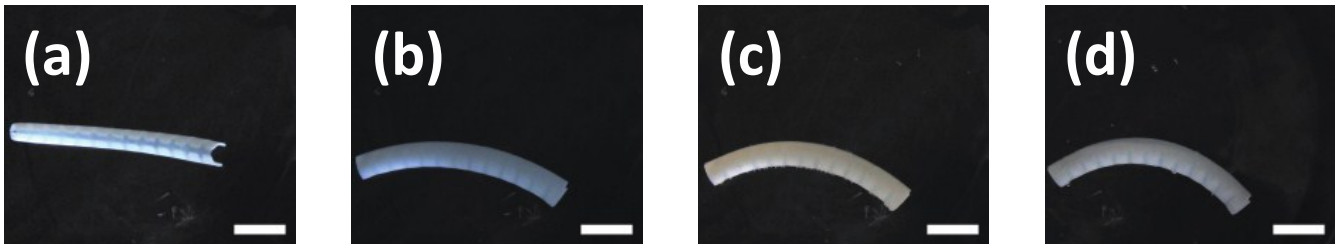

Fig. S3. Evolution of the double curvature shape from a single-curvature shape. The p(AA-*co*-BMA) non-responsive PG sheet is patterned with the transverse lines of temperature-responsive p(AA-*co*-BMA)/p(NIPAM) (BG-1) and the longitudinal stripe of temperature-responsive p(AA-*co*-BMA)/p(NIPAM-*co*-HEAM) (BG-2), each with a different LCST. After incubation of the gel for 8 h in water at 40°C h, it forms a long roll. Figures (a-d) show the change in the long roll structure after incubating it in water at 70°C for (a) 15 sec, (b) 15 min, (c) 30 min, (d) 120 min. The scale bar is 1 mm.

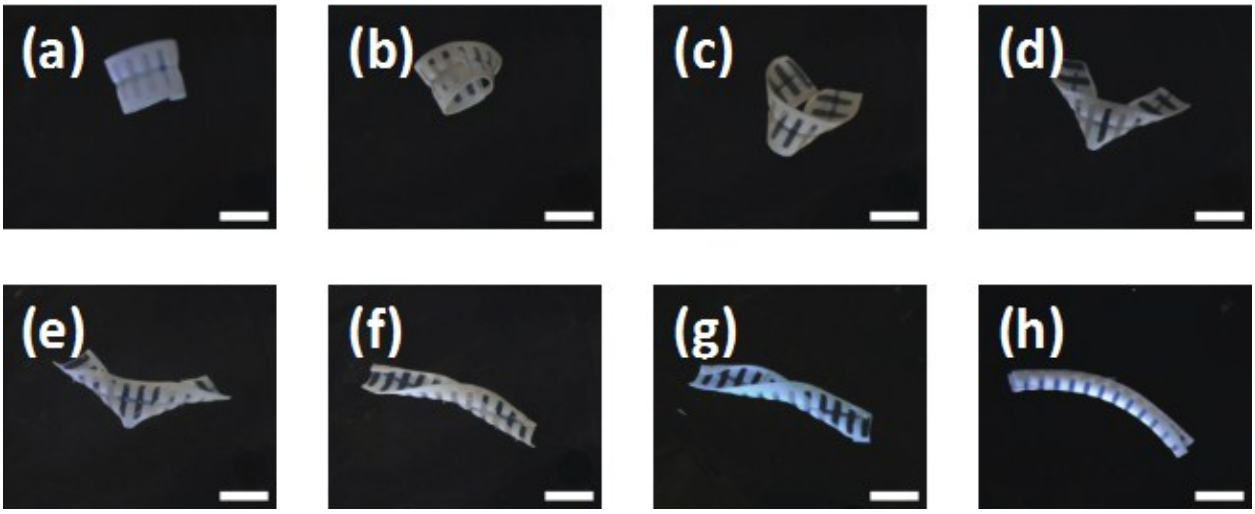

Fig. S4. Evolution of the double curvature shape from a single-curvature shape. The p(AA-*co*-BMA) non-responsive PG sheet is patterned with a longitudinal stripe of temperature-responsive p(AA-*co*-BMA)/p(NIPAM) (BG-1) and the transverse lines of temperature-responsive p(AA-*co*-BMA)/p(NIPAM-*co*-HEAM) (BG-2), each with different LCST. After incubation of the gel for 8 h in water at 40°C h, it forms a short roll. Figures (a-h) show the change in the short roll structure after incubating it in water at 70°C for (a) 15 sec, (b) 12 min, (c) 14 min, (d) 60 min, (e) 90 min, (f) 120 min, (g) 180 min, (h) 900 min. The scale bar is 1 mm.

S3. Numerical simulation

Model. In geometric formulation of elasticity theory, a thin elastic plate is modeled as a two-dimensional (2D) manifold equipped with a reference metric. The reference metric describes the local rest dimensions over the plate. A configuration of the sheet in three-dimensional (3D) space induces the actual metric and a curvature tensor. The elastic energy functional is composed of two terms: (i) a

stretching term, which limits deviations from the reference metric, and (ii) a bending term, which hinders out-of plane deflections. The actual configuration of the plate corresponds to the minimum energy functional.

To model the sheet with a design similar to the experimental one, a relation should be established between the reference metric and the swelling process of the plate patterned with the contracting longitudinal stripe and multiple transverse stripes. In addition, we have to supply a constitutive relation that would define the elastic energy functional.

Before activating the swelling process, the composite gel sheet was uniform and flat, that is, it was described by a Euclidean reference metric. In a Cartesian coordinate system, the reference metric takes the form of

$$\bar{a}_0 = \begin{pmatrix} 1 & 0 \\ 0 & 1 \end{pmatrix} \tag{S.1}$$

In the activated swelling process, the hydrogel sheet expands or shrinks at each point, depending on its composition. As this process is position (location)-dependent, the reference metric changes according to the swelling factor $\bar{a}$ as

$$\bar{a} = f(u,v)^2 \begin{pmatrix} 1 & 0 \\ 0 & 1 \end{pmatrix} \tag{S.2},$$

where $f(u,v)$ is the shrinkage-length-factor, and u,v are the coordinates of a given point of the sheet. For the patterned structure shown in Fig.1, $f(u,v)$ takes constant values on the red regions (PG) and constant larger values on the gray regions (BG) of the hydrogel sheet

The constitutive relation was assumed to be Hookean, that is, the stress changes linearly with the strain. Then, the energy functional takes the form

$$W_{st} = \frac{t}{8} \iint A^{\alpha\beta\gamma\delta} (a - \bar{a})_{\alpha\beta} (a - \bar{a})_{\gamma\delta} \sqrt{|\bar{a}|}\, du\, dv \tag{S.3}$$

$$W_{bn} = \frac{t^3}{12} \iint A^{\alpha\beta\gamma\delta} b_{\alpha\beta} b_{\gamma\delta} \sqrt{|\bar{a}|}\, du\, dv \tag{S.4}$$

$$W = W_{st} + W_{bn} \tag{S.5}$$

Note that the actual metric and curvature tensors a and b are not independent: they are interrelated through the *Gauss theorema egregium.* Assuming that the reference metric of the form described by eq.

S2 and the energy functional form (eqs. S3-S5) completely define the elastic problem, the shape transitions of the gel sheet could be properly modeled.

Simulation. In general, an analytic minimization of the elastic energy functional is a difficult task. Therefore, we undertook a numerical approach. In order to find the 3D configuration of a sheet with a given reference metric, we used a 3D finite element simulation, which models the sheet as a 2D triangular mesh embedded in the 3D Euclidean space. We relate to each triangle elastic properties, that is, the Young's modulus Y and the Poisson's ratio. In addition, we relate the triangles with the values of the reference metric $\bar{a}$**.**

Given a configuration of the triangles or vertices in 3D Euclidean space, we estimate for each triangle its actual metric according to the conformation of the triangle and its neighbors. Similarly, we estimate for each triangle its actual curvature. According to the stretching and bending energy (eqs. S3-4) of each mesh unit, we calculated the elastic energy for each triangle. Then, summing over all the triangles we obtained the total elastic energy of the sheet. Given an initial sheet configuration, we minimized the elastic energy with respect to the vertices coordinates. In this manner, we obtained the actual 3D configuration of the sheet, which corresponded to the minimized the elastic energy functional.

Numerical results

In order to study the shape transitions observed in the experiments, we simulated sheets with a qualitatively similar geometry. We used the freedom of working in dimensionless form, setting $d = 1$, $t = 0.1$, $L = 20$, and $w = 8$, where d and t are the theoretical thicknesses of the lines of PG and the sheet, respectively, and L and w are the theoretical length and width of the sheet, respectively. In order to allow convergence of the simulations, we used the swelling/shrinkage ratios that were lower than the actual ones. The PG length-shrinkage-factor was $\sqrt{0.9}$ and the BG length-expansion-factor was $\sqrt{1.1}$. In addition, the presented data were obtained for the case of uniform Young's modulus and thickness. The assumption of a uniform Young's moduli and thickness may be the one of the reasons of the absence of helical structures in the simulations.

We simulated sheets with different parameters A and p, corresponding to the theoretical amplitude and the spacing of the responsive domains, respectively. We mapped the transitions between single-curvature and double curvature hydrogel shapes, thereby verifying some of experimental findings (see

Fig. 5, main text). Below we present the results for several regimes of the phase-diagram presented in the main text.

The asymptotic (limiting) regimes

The first asymptotic regime (limiting case 1 as in main text) is that of dense transverse stripes (a very small value of p). In this case, as explained in the main text, one can view the system as a single wide longitudinal stripe of width A at the center of the sheet (the outmost left shape below). Other observed configurations for the values of A and $p = d$ are given in Fig. S6a. The variation in curvatures corresponding to these configurations is shown in Fig. S5b.

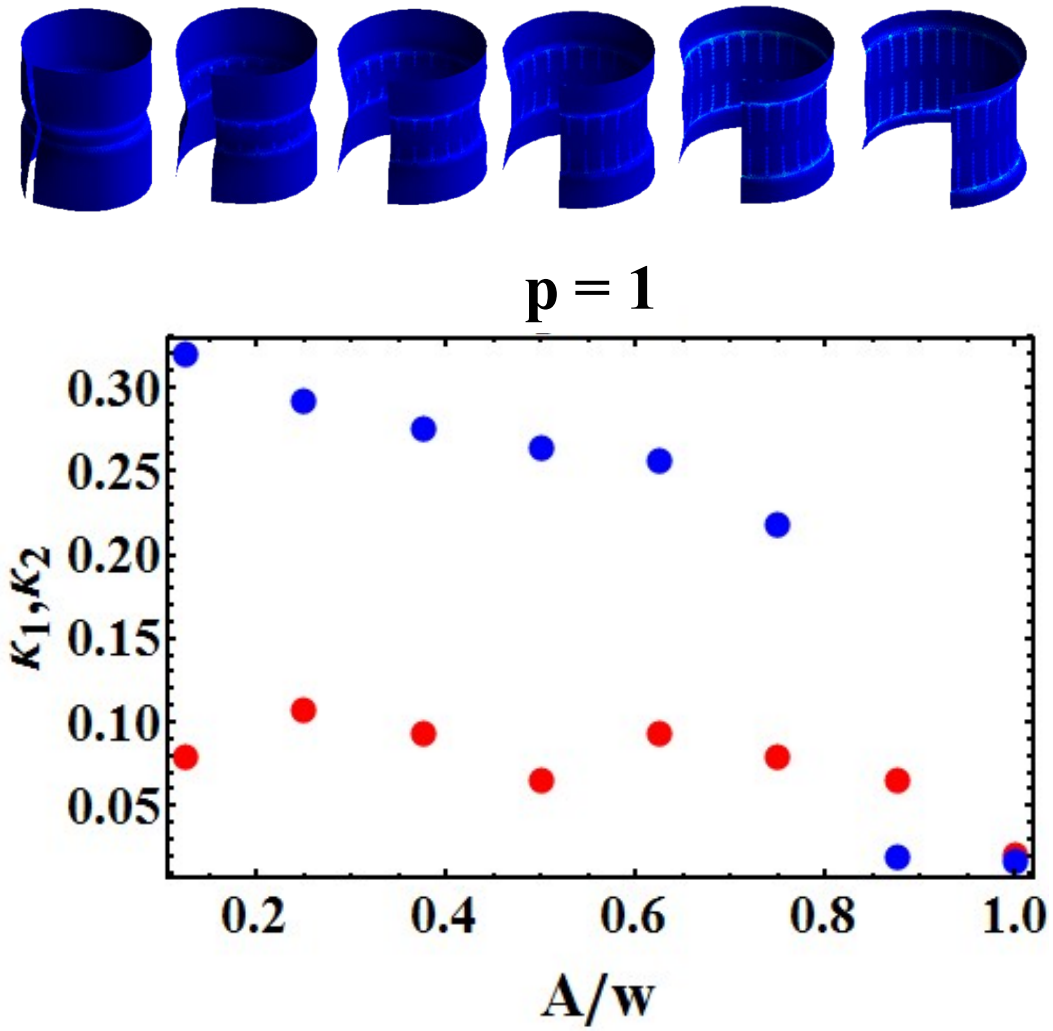

Fig. S5. Configuration variation as a function of modulation amplitude in the small p regime ($p = 1$). (a) Equilibrium configurations of strips with the amplitude A/w increasing from left to right ($\frac{1}{8}, \frac{2}{8}, \frac{3}{8}, \frac{4}{8}, \frac{5}{8}$ and $\frac{6}{8}$). (b) The principal curvatures of the configurations in (a). The colors indicate the elastic (dimensionless) energy density.

Another asymptotic regime is that of distant transverse stripes (limiting case 2). In this case, as explained in the main text, the effect of the transverse stress is negligible and we find the following set of equilibrium configurations of the sheet

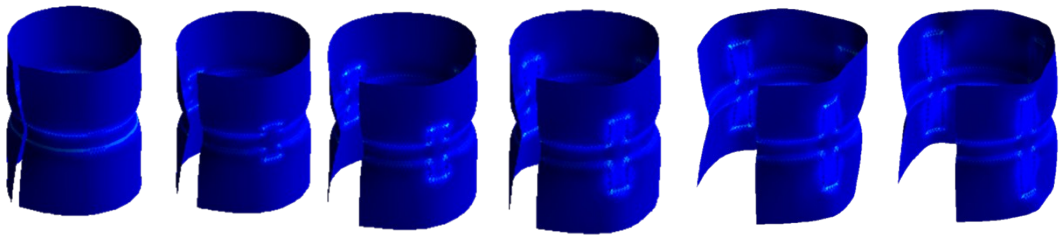

Fig. S6. Configuration variation as a function of modulation amplitude in the large p regime $(p = 6)$. Equilibrium configurations of strips with the amplitude A/w increasing from left to right $(\frac{1}{8}, \frac{2}{8}, \frac{3}{8}, \frac{4}{8}, \frac{5}{8} \; and \; \frac{6}{8})$. The colors indicate the elastic (dimensionless) energy density.

Intermediate regimes

A richer behavior is observed for the intermediate regimes. In the case of $p = 3.5$ and $1 \leq A \leq 8$, a transition from a short roll to long roll through a double curvature configuration is observed, as shown in Fig. S7a. By using a numeric fitting procedure, we extracted from the configurations the radius of the longitudinal and transverse curvatures, obtaining the results shown in Fig. S7b.

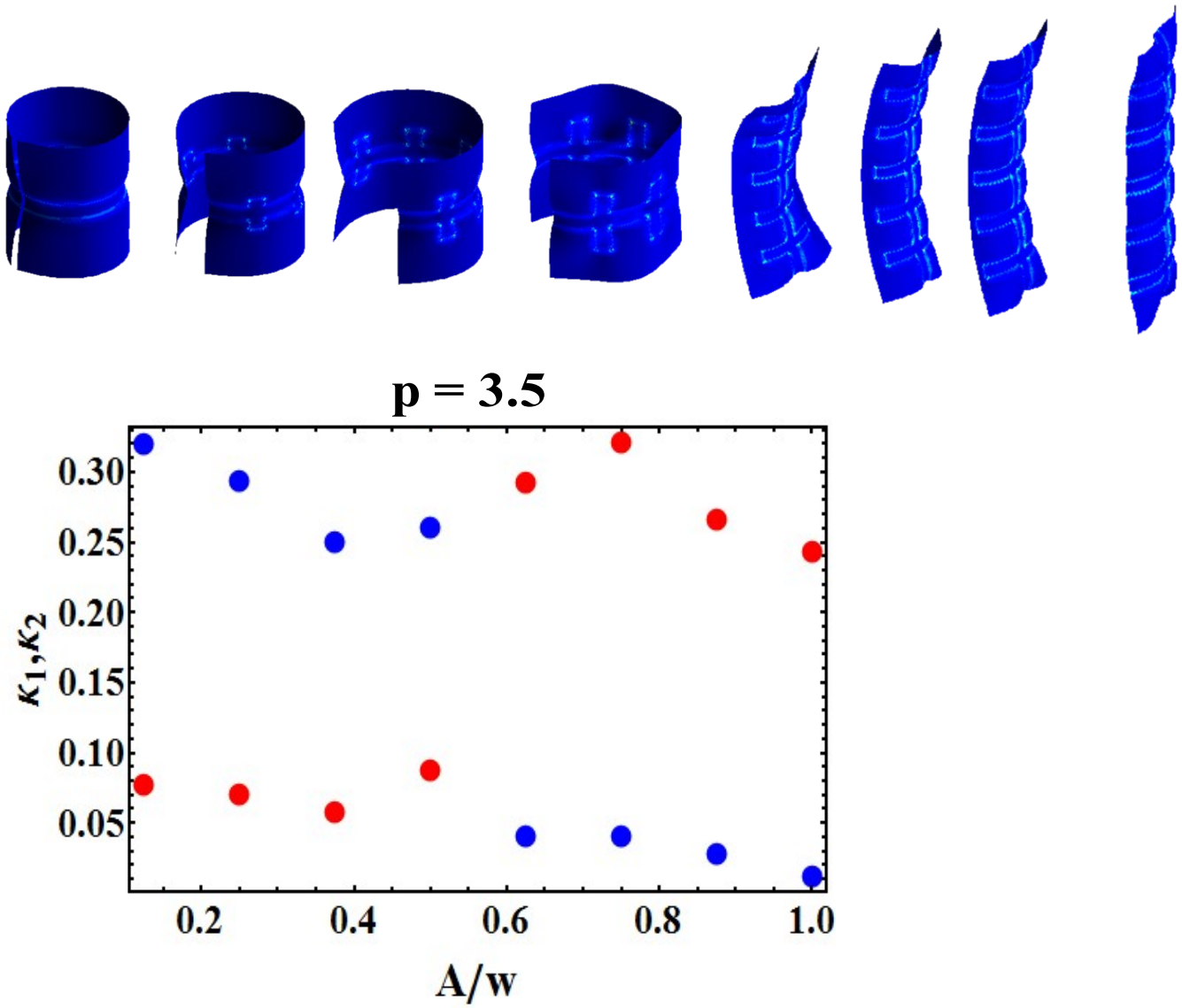

Fig. S7. Configuration variation as a function of modulation amplitude in the intermediate regime ($p = 3.5$). (a) Equilibrium configurations of strips with the amplitude A/w increasing from left to right ($\frac{1}{8}, \frac{2}{8}, \frac{3}{8}, \frac{4}{8}, \frac{5}{8}, \frac{6}{8}, \frac{7}{8}$ *and* 1). The colors indicate the elastic (dimensionless) energy density. (b) The principal curvatures of the configurations in (a).